https://ntrs.nasa.gov/search.jsp?R=19950019493 2020-06-16T07:34:21+00:00Z

19951194 93

N95-25913

44626

p. 22

APPENDIX B

SUMMARY OF LET SPECTRA AND DOSE MEASUREMENTS ON TEN STS MISSIONS

Introduction

The dosimetry performed on STS flights includes Area Passive Dosimeters (APDs) and Crew Passive Dosimeters (CPDs). Each dosimeter type contains plastic nuclear track detectors (PNTDs) for the measurement of LET spectra of heavy particles ($LET_{\infty} \cdot H_2O \geq 5$ keV/μm). For purposes of mission intercomparisons, or of comparisons with model calculations or other measurements, the APDs yield more consistent results. The PNTD stacks are directional in response. The APDs contain three orthogonal stacks to average over solid angle. The CPDs, which are carried by astronauts in a breast pocket, depend on the movement of the crew about the Shuttle to average over solid angles. Also the APDs have been mounted in the same locker location and orientation for all recent missions. For this reason a selection of APD PNTDs have been read out to provide LET data for missions with different flight parameters.

Flight Dosimetry

The APD dosimetry results reported here are for the STS-37, -39, -40, -41, -42, -43, -44, -45, -48 and -50 missions. The APDs were located in Locker MF71C in the Shuttle crew compartment, except for STS-42 in which results were derived from a portion of the RME APD. Each of the three orthogonal PNTD stacks consisted of a CR-39 doublet (two sheets of film with dimensions of 4.5 cm x 3.0 cm x 0.06 cm) separated by an 8 μm-thick film of polycarbonate plastic.

After return of the flight dosimeters, the CR-39 PNTDs were processed by the standard method to delineate latent particle tracks. The readout of the PNTDs requires a scanning procedure to locate tracks in the surfaces of the CR-39 followed by measurement of individual track parameters. Particle LET is calculated from the lengths of the major and minor axes of elliptical track

openings, depths of material etched from the CR-39 surfaces and calibration curves of PNTD sensitivity versus particle LET. The calibration curves are constructed from a series of measurements with accelerated particles of known LET.

Automated Readout of PNTDs

Readout of PNTDs is carried out on the automated scanning and measurement SAMAICA systems at The University of San Francisco. SAMAICA is an acronym for Scanning and Measuring with Automated Image Contour Analysis and is a product of ELBEK GmbH in Siegen, Germany. The system performs a fully automated scan of CR-39 PNTDs for track detection and then incorporates interactive modes for track classification and measurement. The classification involves an examination of the four surfaces of an assembled CR-39 doublet by the system operator to determine whether the particle was long range (creating four colinear tracks at the surfaces) or short range (creating 2 or 3 colinear tracks). In all cases the particle was required to create a track pair at the adjacent (#2, #3) surfaces of the doublet.

After classification the tracks on surface #3 of the doublet were measured. (The system software makes an initial fit of an ellipse to the track opening, then allows the operator to manually adjust the fit.) The measurement data were then reduced to integral and differential LET spectra with standard analysis software developed at USF. Data from the three orthogonal (x, y, z) stacks were combined into average LET spectra.

Measurements

Integral LET flux spectra for the ten missions listed above are shown in Figures 1 to 10. Shown are curves for long range (>1200 μm) and short range tracks (80 to 1200 μm) with a total curve shown in each case for both flux components added together. Long range particles are likely to be galactic cosmic rays and projectile secondaries, while short range particles are probably stopping primary particles plus secondaries from target nuclei. At the highest Shuttle altitudes the short range particles are dominated by the contribution from trapped particles in the Earth's magnetic field, mainly protons. The lower LET detector threshold

in each case is approximately 5 keV/μm. Relevant information for each flight concerning flux, dose-rate, dose-equivalent rate and total dose is given in Tables 1-10. The dose equivalent rate is determined by weighting particle LET fluxes by Quality Factors from ICRU 19 (1971).

Discussion

As can be seen from the integral flux plots, the contribution to total flux from short range tracks is, as expected, greater than that for long range tracks, for all altitudes and inclinations. At high altitudes the contribution is dominated by trapped protons. The short registration range of protons in CR-39 (~1000 μm) ensures that most of this contribution (stopping primary and secondary protons) are classified as short range. At lower altitudes, and especially at higher inclinations, the galactic cosmic rays (which produce the long range tracks) become more important. However, most of the GCRs have LETs <5 keV/μm, the sensitivity limit of CR-39. Their contributions to the LET spectra come through nuclear reactions and the production of target secondary particles, which are classified as short range. Even at very low altitude and high inclination orbits, the CR-39 detects a large fraction of short range particles.

When the flux spectra are converted to dose rates a different picture emerges. The long range particles tend to be higher in LET than short range particles and they become relatively more important. The contribution of long range particles to total dose is given by the long range dose ratio defined as (long range dose)/(total dose) and is given in Table 11 for each flight. As can be seen from this table, the long range dose ratio seems to increase with inclination, with the ratio being greatest for relatively low altitude (approx. 290 km), high inclination (57°) orbits. However, the ratio for STS-48 was 0.207 which is due to the fact that this flight had an altitude of 565 km and therefore cut across Earth's inner radiation belt at the South Atlantic Anomaly, hence registering a greater percentage of short range particles. Since the lowest and highest altitudes for a given

inclination of 57° in this report were for flights STS-39 and STS-48, the effect of changing the orbital altitude can clearly be seen, with ratios of 0.578 and 0.207 respectively. The dose ratio for the 28° inclination orbit is variable but decreases with orbital altitude. In general the dose ratio is much lower for 28° orbits for two reasons: the magnetic field cutoff for GCRs extends to higher particle energies and the Shuttle spends a greater fraction of orbital time within the SAA.

Figure 11 is a plot of dose equivalent rate against altitude and inclination, therefore enabling a general inter-comparison of dose equivalents to be made. The dose equivalent rate tends to increase with both altitude and inclination. There are significant variations within this relationship, however. For instance, the STS-44 dose equivalent appears higher than would be expected while that for STS-37 is less. It is interesting to note that the crew average total dose rates for these missions, as measured with TLDs by Johnson Spaceflight Center personnel, are 0.294 mGy d^{-1} on STS-37 and 0.094 mGy d^{-1} for STS-44. These dose rates are much as expected from the orbital parameters. This demonstrates that the high LET portion of cosmic radiation (>5 keV/μm) is much more variable than total dose, which is dominated by more penetrating low LET radiation. The differences can arise from effective shielding variations between missions (different Shuttle contents or different orientations with respect to the directions of maximum incoming radiation). The dose rate of particles >5 keV/μm is only 5.6% of total crew dose rate for STS-37 and 29% of total for STS-44. These dose rate fractions are near the extreme lower and upper boundaries which have been measured with PNTDs on Shuttle missions.

TABLES

Tables 1-11: Data concerning dose ratios, altitudes and inclinations for each of the flights indicated below (see Figure Captions).

FIGURE CAPTIONS

Figure 1: Integral LET flux spectra for the STS-37 APDs.
Figure 2: Integral LET flux spectra for the STS-39 APDs.
Figure 3: Integral LET flux spectra for the STS-40 APDs.
Figure 4: Integral LET flux spectra for the STS-41 APDs.
Figure 5: Integral LET flux spectra for the STS-42 APDs.
Figure 6: Integral LET flux spectra for the STS-43 APDs.
Figure 7: Integral LET flux spectra for the STS-44 APDs.
Figure 8: Integral LET flux spectra for the STS-45 APDs.
Figure 9: Integral LET flux spectra for the STS-48 APDs
Figure 10: Integral LET flux spectra for the STS-50 APDs
Figure 11: Plot of dose equivalent rate against altitude and inclination for all flights presented in this report.

Table 1: STS 37 APD DOSE TABLE

For LET$\geq 5 KeV/\mu m$

	FLUX ($cm^{-2}s^{-1}sr^{-1}$)	DOSE RATE ($mrad\ day^{-1}$)	DOSE EQUIV. RATE ($mrem\ day^{-1}$)	TOTAL DOSE EQUIV. ($mrem$)
TOTAL	1.004×10^{-3}	2.534	14.310	85.631
LR	4.943×10^{-5}	0.165	1.297	7.761
SR	9.548×10^{-4}	2.374	13.012	77.864

Table 2: STS 39 APD DOSE TABLE

For LET$\geq 5 KeV/\mu m$

	FLUX ($cm^{-2}s^{-1}sr^{-1}$)	DOSE RATE ($mrad\ day^{-1}$)	DOSE EQUIV. RATE ($mrem\ day^{-1}$)	TOTAL DOSE EQUIV. ($mrem$)
TOTAL	6.267×10^{-4}	1.853	14.039	116.62
LR	1.869×10^{-4}	0.670	6.872	57.086
SR	4.582×10^{-4}	1.183	7.166	59.528

Table 3: STS 40 APD DOSE TABLE

For LET$\geq 5 KeV/\mu m$

	FLUX ($cm^{-2}s^{-1}sr^{-1}$)	DOSE RATE ($mrad\ day^{-1}$)	DOSE EQUIV. RATE ($mrem\ day^{-1}$)	TOTAL DOSE EQUIV. ($mrem$)
TOTAL	2.611×10^{-4}	0.687	5.095	46.332
LR	8.139×10^{-5}	0.233	1.916	17.424
SR	1.797×10^{-4}	0.454	3.178	28.900

Table 4: STS 41 APD DOSE TABLE

For LET$\geq 5 KeV/\mu m$

	FLUX ($cm^{-2}s^{-1}sr^{-1}$)	DOSE RATE ($mrad\ day^{-1}$)	DOSE EQUIV. RATE ($mrem\ day^{-1}$)	TOTAL DOSE EQUIV. ($mrem$)
TOTAL	1.148×10^{-3}	2.914	15.671	64.047
LR	4.090×10^{-5}	0.156	1.621	6.625
SR	1.107×10^{-3}	2.758	14.051	57.426

Table 5: STS 42 APD DOSE TABLE

For LET$\geq 5 KeV/\mu m$

	FLUX ($cm^{-2}s^{-1}sr^{-1}$)	DOSE RATE ($mrad\ day^{-1}$)	DOSE EQUIV. RATE ($mrem\ day^{-1}$)	TOTAL DOSE EQUIV. ($mrem$)
TOTAL	7.859×10^{-4}	2.005	14.587	117.45
LR	3.890×10^{-4}	0.961	7.820	62.970
SR	4.043×10^{-4}	1.044	6.767	54.490

Table 6: STS 43 APD DOSE TABLE

For LET$\geq 5 KeV/\mu m$

	FLUX ($cm^{-2}s^{-1}sr^{-1}$)	DOSE RATE ($mrad\ day^{-1}$)	DOSE EQUIV. RATE ($mrem\ day^{-1}$)	TOTAL DOSE EQUIV. ($mrem$)
TOTAL	8.061×10^{-4}	2.135	12.942	115.050
LR	3.220×10^{-4}	0.549	2.882	25.620
SR	4.840×10^{-4}	1.586	10.060	89.433

Table 7: STS 44 APD DOSE TABLE

For LET$\geq 5 KeV/\mu m$

	FLUX ($cm^{-2}s^{-1}sr^{-1}$)	DOSE RATE ($mrad\ day^{-1}$)	DOSE EQUIV. RATE ($mrem\ day^{-1}$)	TOTAL DOSE EQUIV. ($mrem$)
TOTAL	1.675×10^{-3}	5.559	36.490	253.64
LR	8.894×10^{-5}	0.345	2.740	19.046
SR	1.586×10^{-3}	5.214	33.752	234.61

Table 8: STS 45 APD DOSE TABLE

For LET$\geq 5 KeV/\mu m$

	FLUX ($cm^{-2}s^{-1}sr^{-1}$)	DOSE RATE ($mrad\ day^{-1}$)	DOSE EQUIV. RATE ($mrem\ day^{-1}$)	TOTAL DOSE EQUIV. ($mrem$)
TOTAL	7.587×10^{-4}	2.271	16.051	143.239
LR	2.939×10^{-4}	0.940	8.096	72.249
SR	4.647×10^{-4}	1.331	7.954	70.981

Table 9: STS 48 APD DOSE TABLE

For LET$\geq 5 KeV/\mu m$

	FLUX ($cm^{-2}s^{-1}sr^{-1}$)	DOSE RATE ($mrad\ day^{-1}$)	DOSE EQUIV. RATE ($mrem\ day^{-1}$)	TOTAL DOSE EQUIV. ($mrem$)
TOTAL	5.708×10^{-3}	14.122	75.024	401.53
LR	2.003×10^{-3}	3.749	17.587	94.12
SR	3.705×10^{-3}	10.375	57.438	307.41

Table 10: STS 50 APD DOSE TABLE

For LET$\geq 5 KeV/\mu m$

	FLUX ($cm^{-2}s^{-1}sr^{-1}$)	DOSE RATE ($mrad\ day^{-1}$)	DOSE EQUIV. RATE ($mrem\ day^{-1}$)	TOTAL DOSE EQUIV. ($mrem$)
TOTAL	6.944×10^{-4}	2.578	20.723	286.25
LR	1.403×10^{-4}	0.441	4.694	64.838
SR	5.635×10^{-4}	2.138	16.029	221.41

Table 11: LONG RANGE DOSE EQUIV. RATIO FOR EACH STS FLIGHT

STS NO.	ALTITUDE (km)	INCLINATION ($degrees$)	LONG RANGE DOSE EQUIV. RATIO
37	450	28.5	9.06×10^{-2}
44	361	28.5	7.51×10^{-2}
43	296	28.5	2.23×10^{-1}
50	296	28.45	2.27×10^{-1}
41	291	28.5	1.03×10^{-1}
40	296	39.0	3.76×10^{-1}
48	565	57.0	2.34×10^{-1}
42	302	57.0	5.36×10^{-1}
45	296	57.0	5.04×10^{-1}
39	263	57.0	4.90×10^{-1}

INTEGRAL LET-SPECTRA (FLUX)

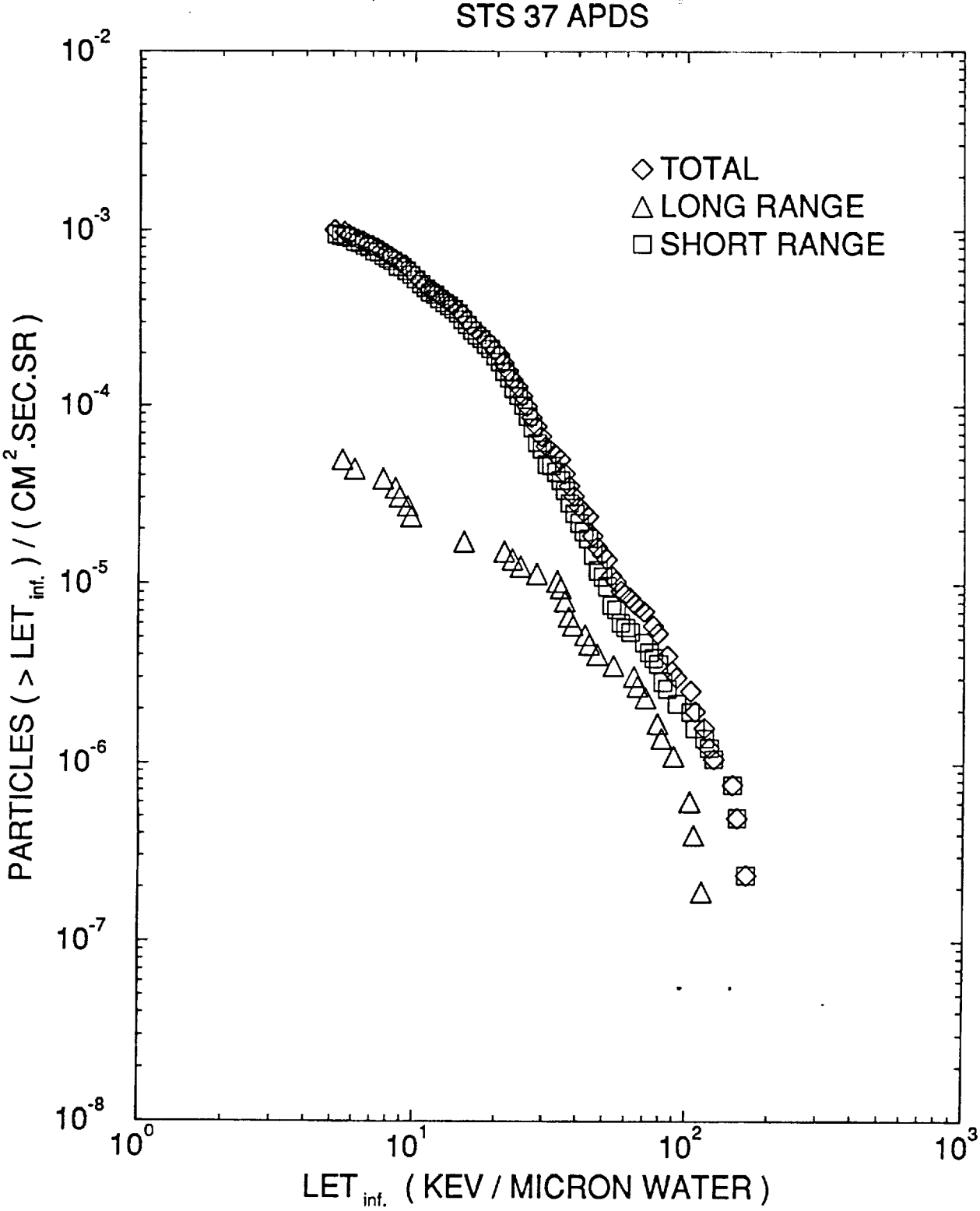

FIGURE B1

INTEGRAL LET-SPECTRA (FLUX)

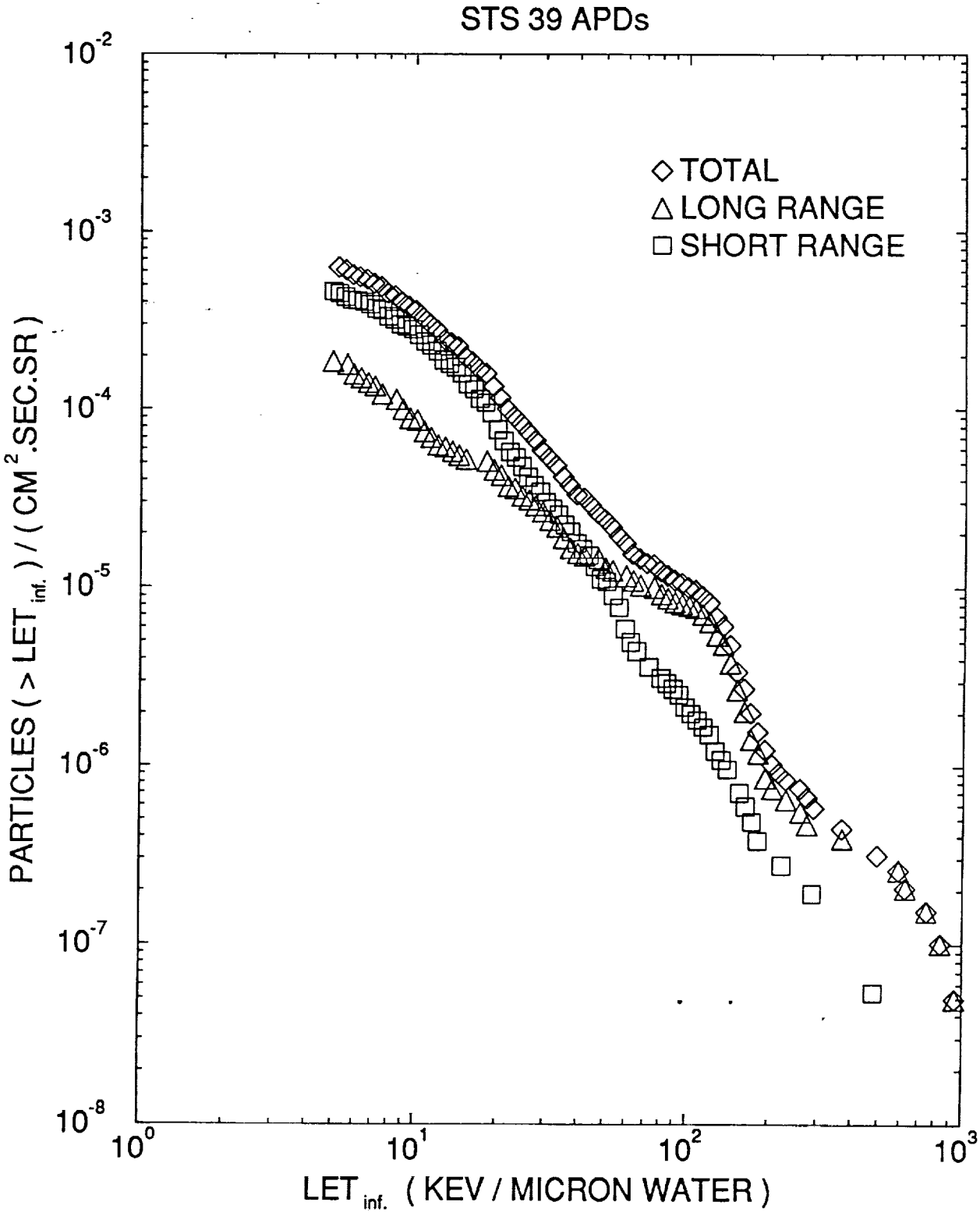

FIGURE B2

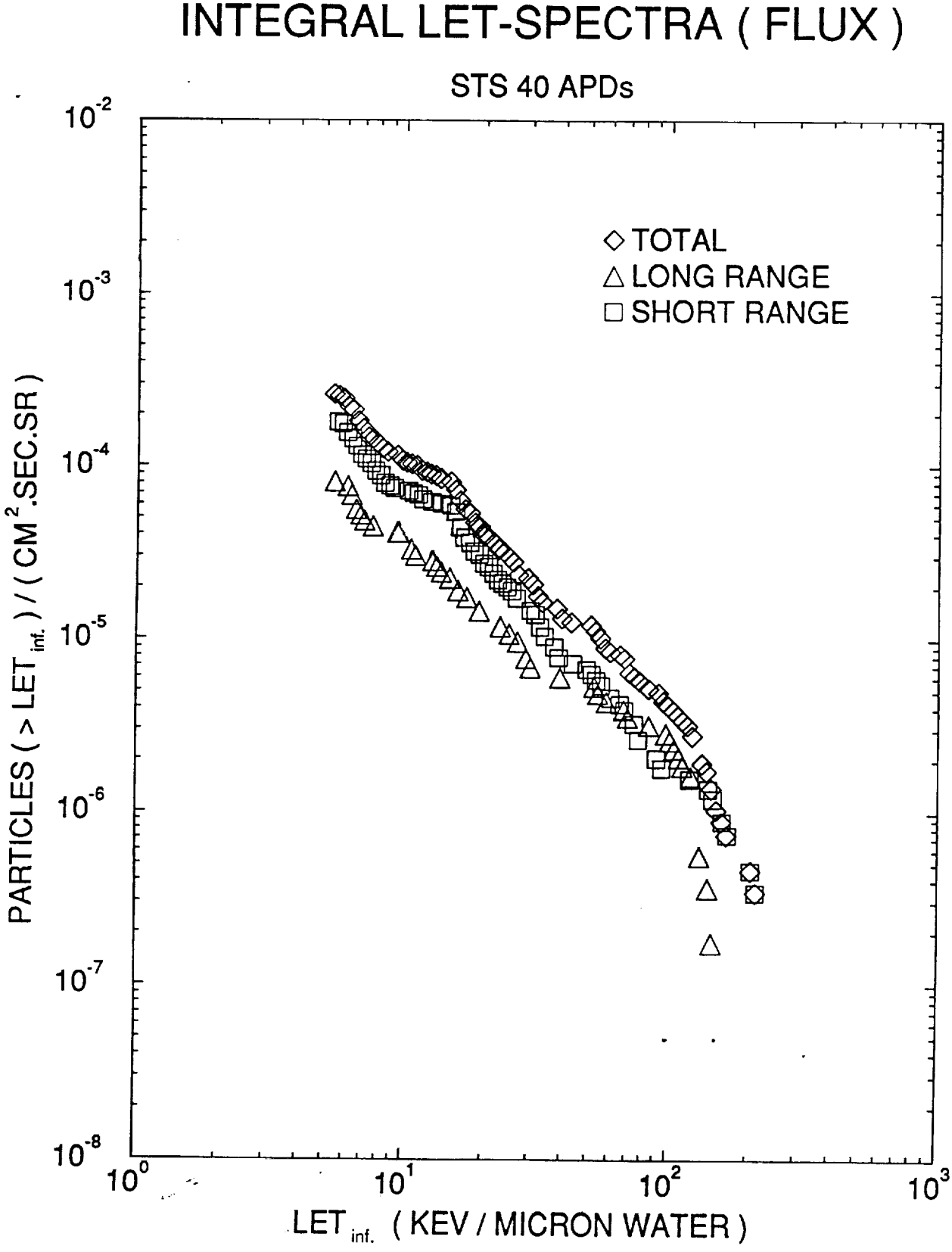
INTEGRAL LET-SPECTRA (FLUX)
STS 40 APDs
◇ TOTAL
△ LONG RANGE
□ SHORT RANGE
PARTICLES (> LET inf.) / (CM2.SEC.SR)
LET inf. (KEV / MICRON WATER)
10-2
10-3
10-4
10-5
10-6
10-7
10-8
100
101
102
103

FIGURE B3

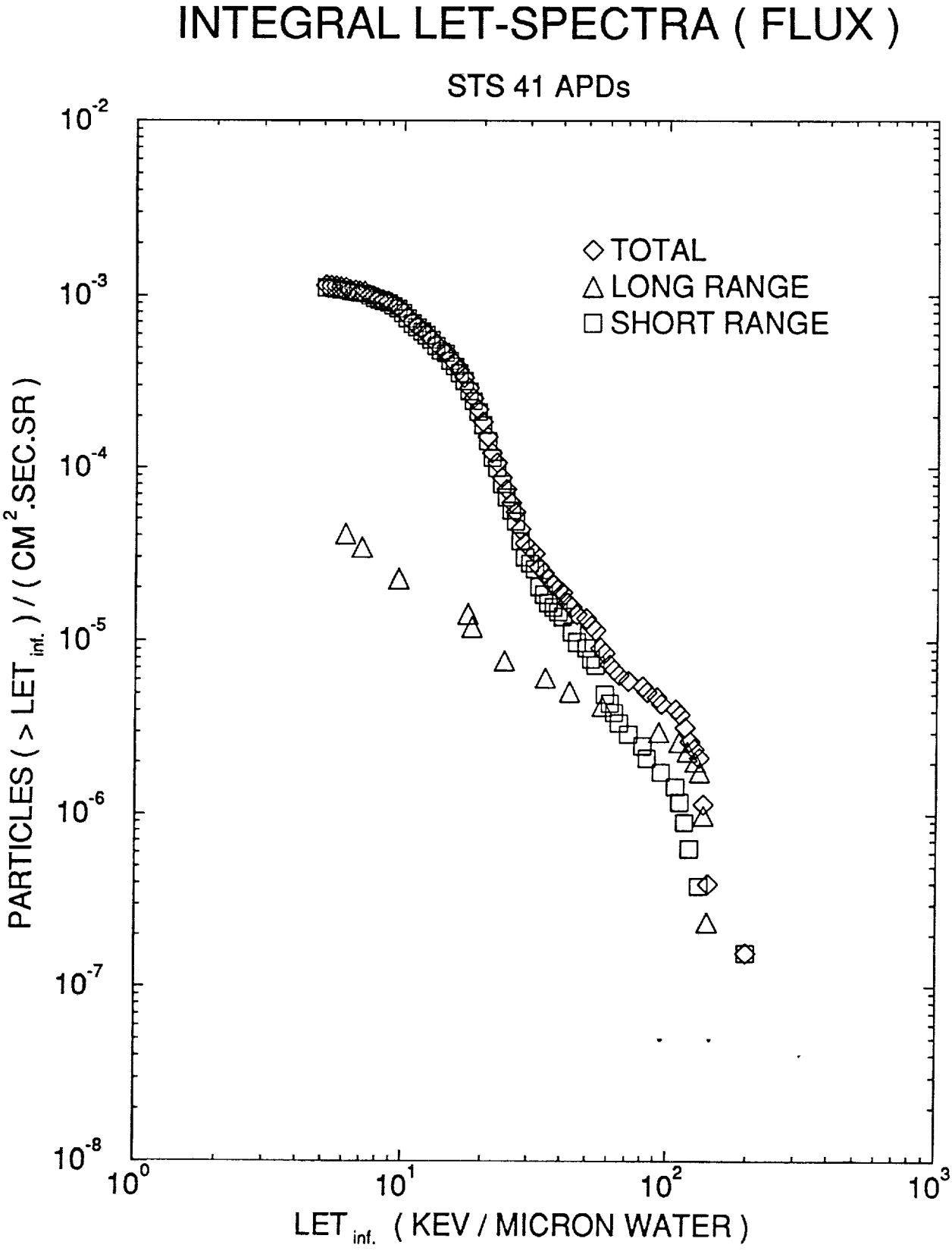
INTEGRAL LET-SPECTRA (FLUX)
STS 41 APDs
◇ TOTAL
△ LONG RANGE
□ SHORT RANGE
PARTICLES (> LET inf.) / (CM 2 .SEC.SR)
LET inf. (KEV / MICRON WATER)
10-2
10-3
10-4
10-5
10-6
10-7
10-8
100
101
102
103

FIGURE B4

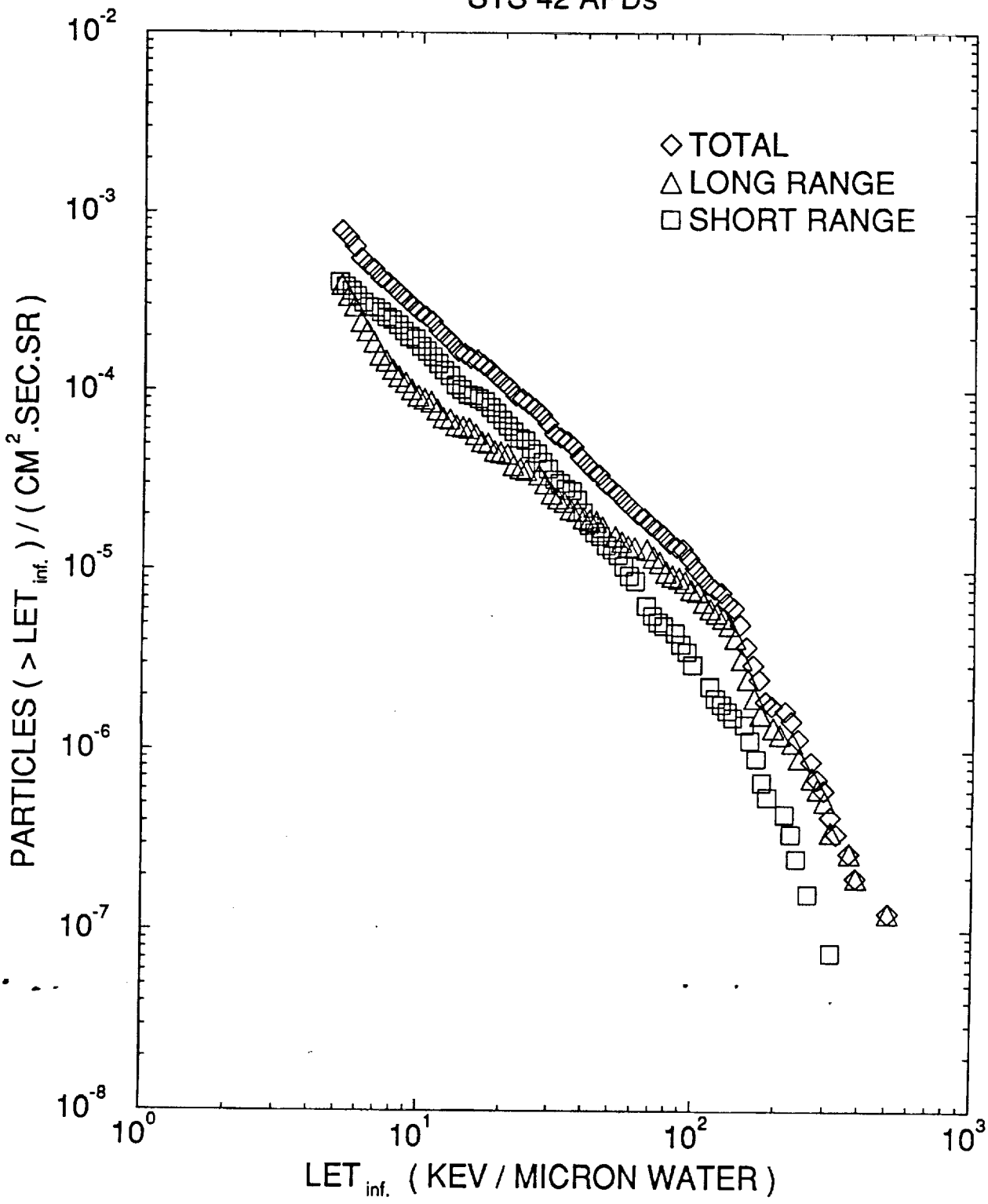
INTEGRAL LET-SPECTRA (FLUX)
STS 42 APDs
◇ TOTAL
△ LONG RANGE
□ SHORT RANGE
PARTICLES (> LET inf.) / (CM 2 .SEC.SR)
LET inf. (KEV / MICRON WATER)
10-2
10-3
10-4
10-5
10-6
10-7
10-8
100
101
102
103

FIGURE B5

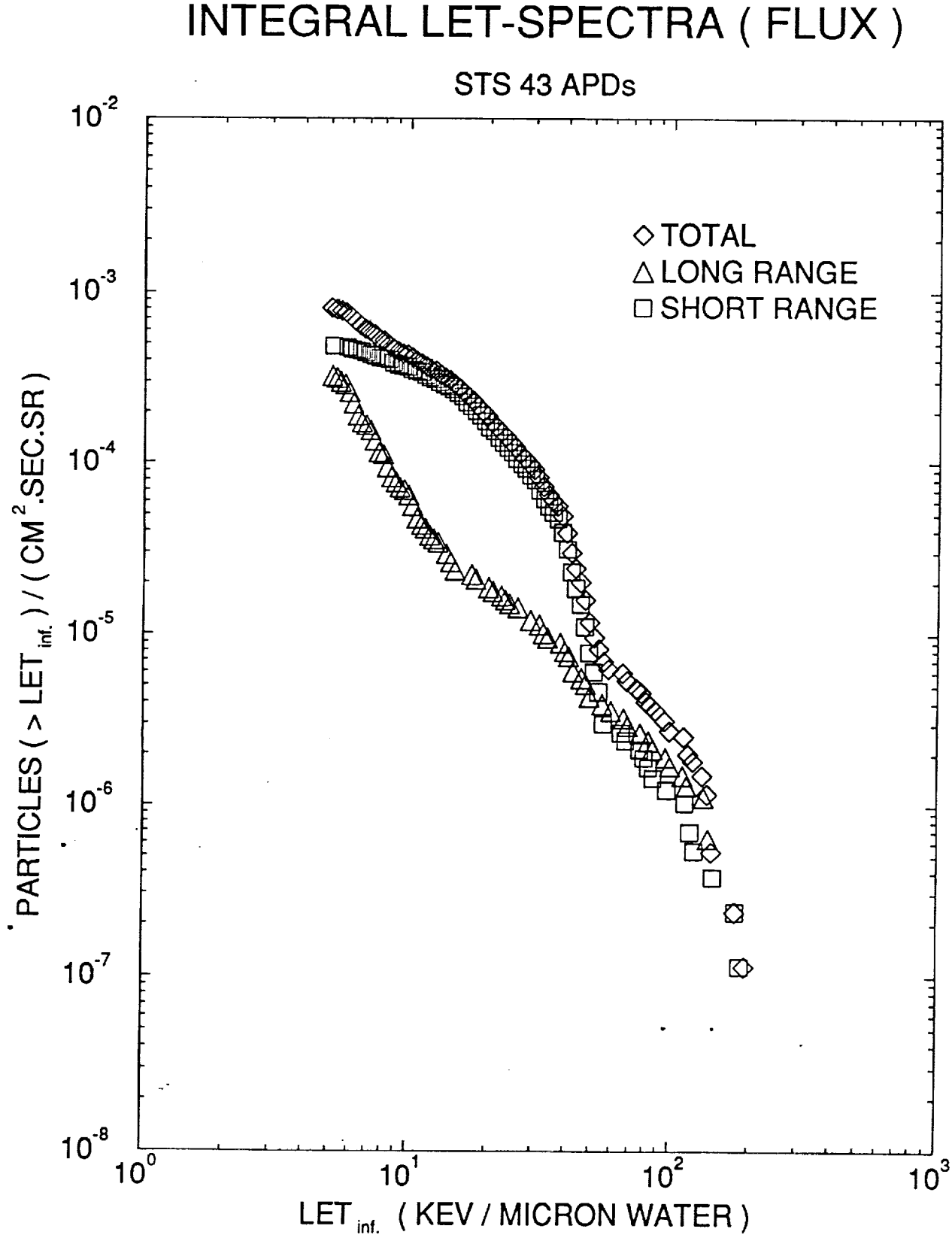
INTEGRAL LET-SPECTRA (FLUX)
STS 43 APDs
TOTAL
LONG RANGE
SHORT RANGE
PARTICLES (> LET inf.) / (CM 2 .SEC.SR)
LET inf. (KEV / MICRON WATER)
10-2
10-3
10-4
10-5
10-6
10-7
10-8
100
101
102
103

FIGURE B6

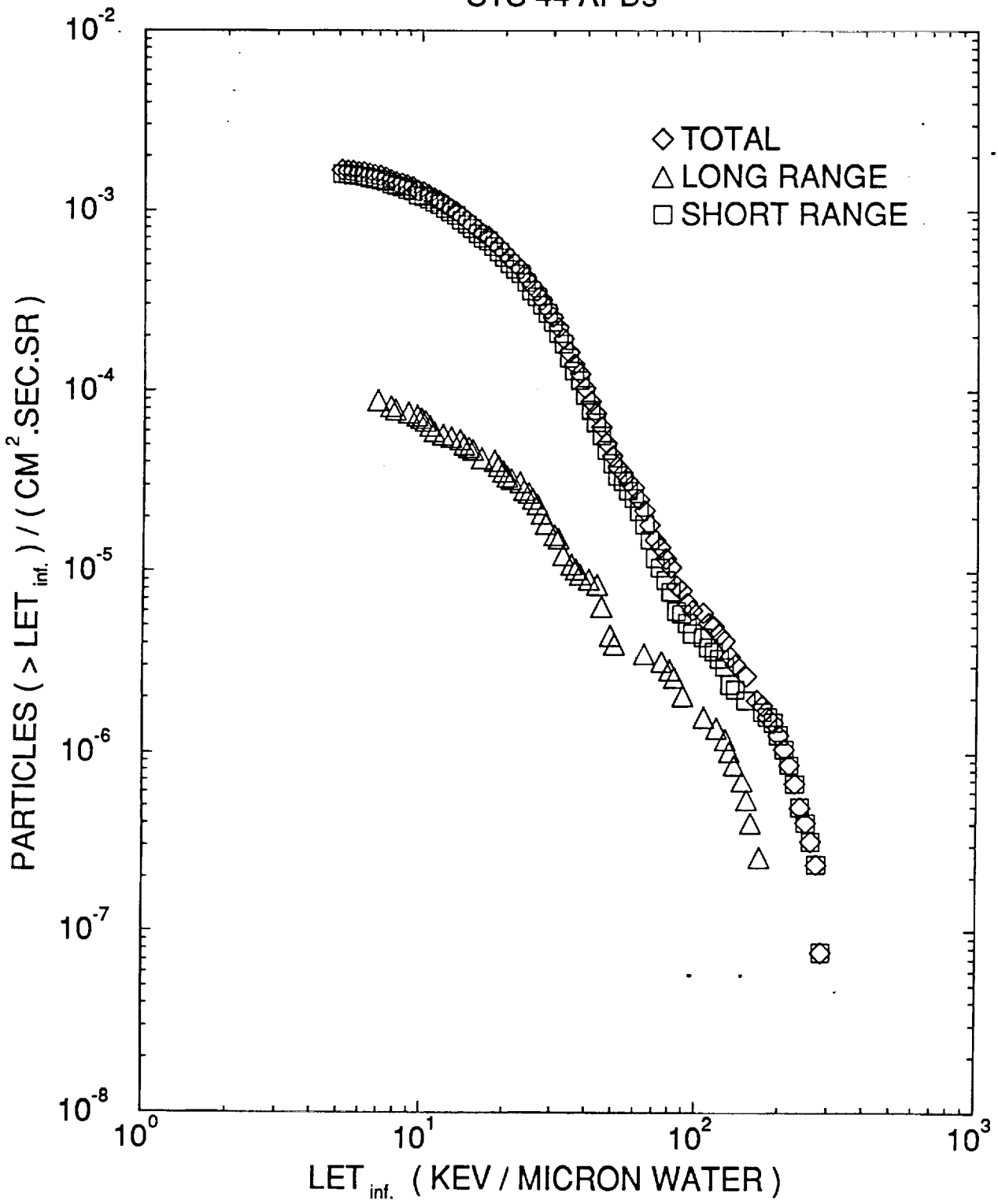
INTEGRAL LET-SPECTRA (FLUX)
STS 44 APDs
◇ TOTAL
△ LONG RANGE
□ SHORT RANGE
PARTICLES (> LET inf.) / (CM 2 .SEC.SR)
LET inf. (KEV / MICRON WATER)
10-2
10-3
10-4
10-5
10-6
10-7
10-8
10 0
10 1
10 2
10 3

FIGURE B7

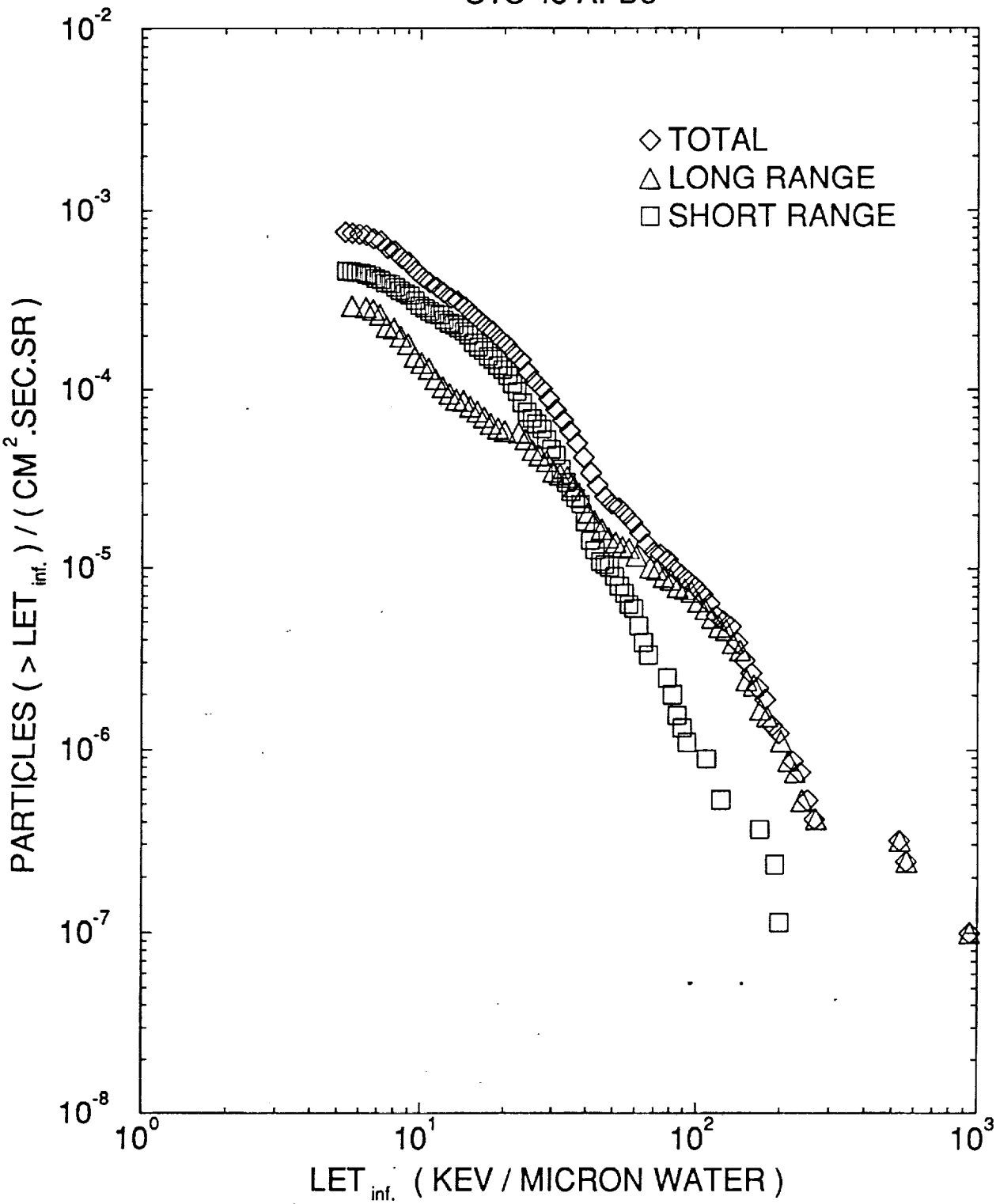
INTEGRAL LET-SPECTRA (FLUX)
STS 45 APDs
◇ TOTAL
△ LONG RANGE
□ SHORT RANGE
PARTICLES (> LET inf.) / (CM 2 .SEC.SR)
LET inf. (KEV / MICRON WATER)
10-2
10-3
10-4
10-5
10-6
10-7
10-8
100
101
102
103

FIGURE B8

INTEGRAL LET-SPECTRA (FLUX)

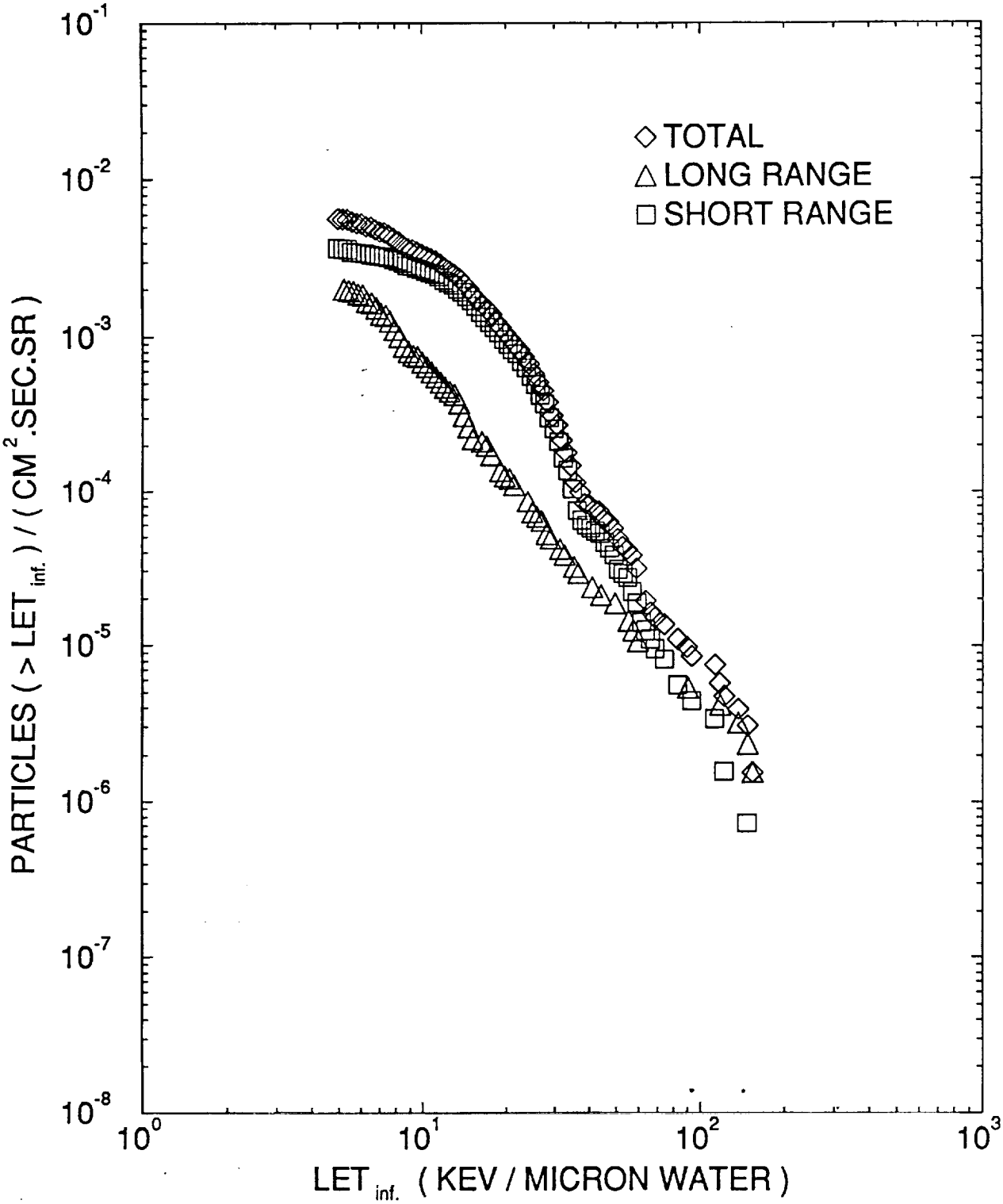

FIGURE B9

INTEGRAL LET-SPECTRA (FLUX)

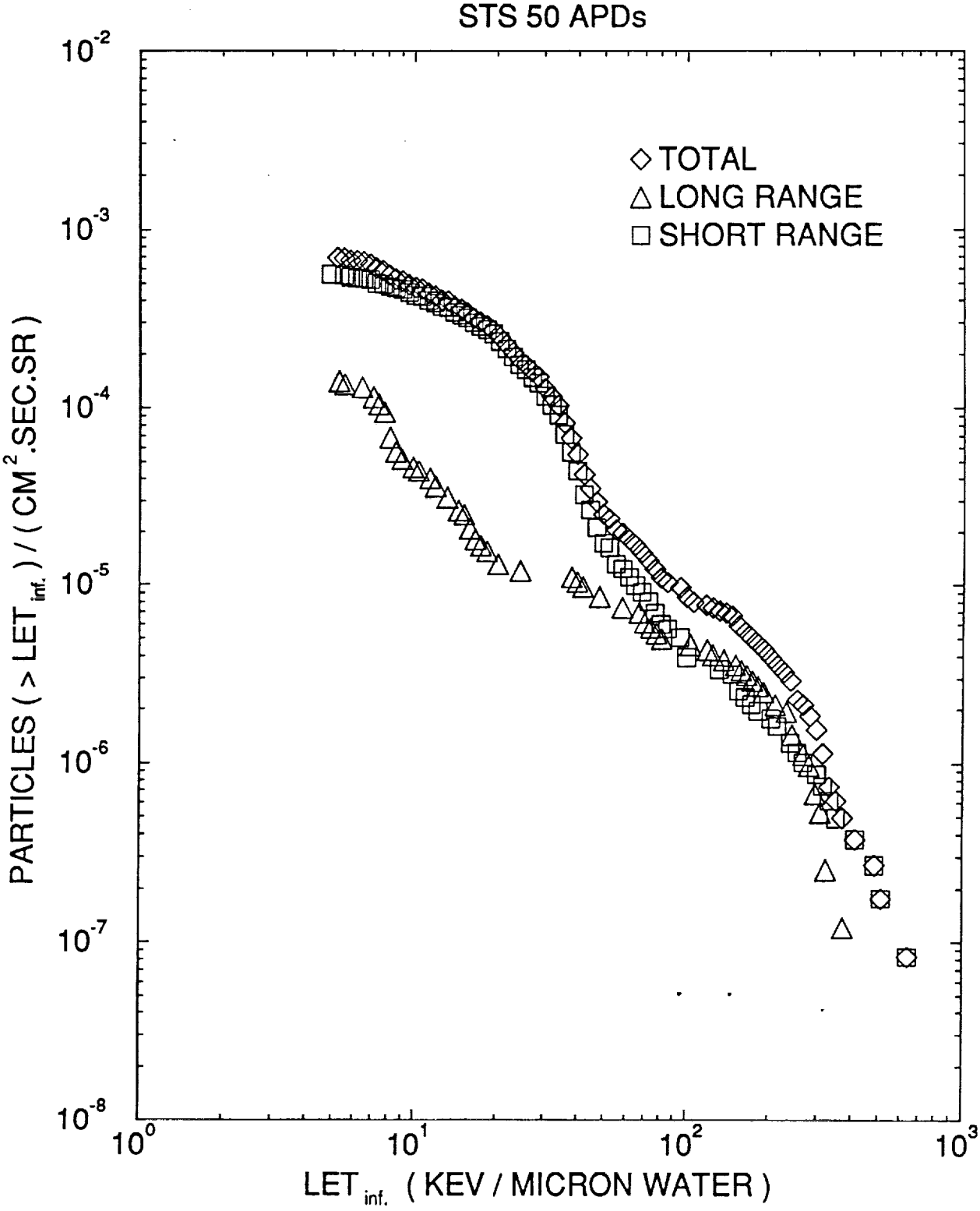

FIGURE B10

DOSE EQUIVALENT RATE PLOT FOR STS FLIGHTS 37,39,40,41,42,43,44,45,48 AND 50

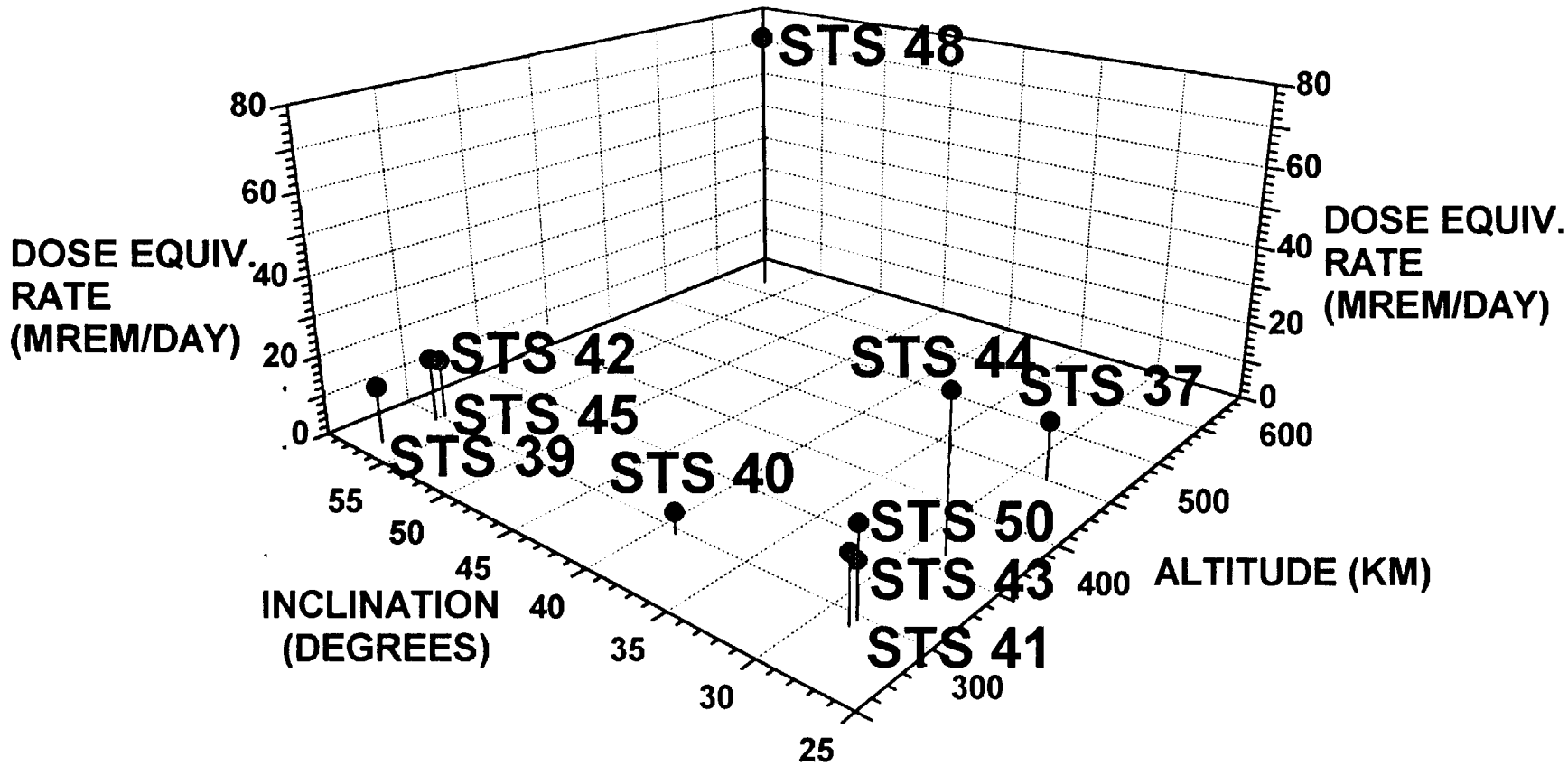

FIGURE B11